Critical analysis of the *T*-history method: a fundamental approach

Heinrich Badenhorst[1,*], Luisa F. Cabeza[2]

[1]*Department of Chemical Engineering, University of Pretoria, Lynnwood Road, Pretoria, 0083, South Africa*

[2]*GREA Innovació Concurrent, Universitat de Lleida, Edifici CREA, Pere de Cabrera s/n, 25001 Lleida, Spain.*

*Corresponding autor: Heinrich.Badenhorst@up.ac.za

Abstract

Energy storage is a key challenge to a sustainable energy supply. To design new storage systems accurate and representative thermal property measurements are essential. The *T*-history method is quick and uncomplicated, however numerous adaptations have been proposed over the years. In this study these methods have been classified and critically assessed based on their mathematical formulation and experimental configuration. They can be broadly categorized according to one of three assumptions regarding the heat transfer coefficient for natural convection: it is constant either as a function of time or temperature, or it is negligible. This work proves in addition that the heat transfer coefficient for natural convection, varies both as a function of time and temperature. This is demonstrated both experimentally and through rigorous simulation of the proposed configurations. Thus *T*-history methods which show the most promise for precise and unambiguous measurements eliminate convection by making conduction the dominant thermal resistance in the system. These techniques can be tailored to different materials and do not require a simultaneous reference due to the use of a rigorous fundamental model compared to the lumped parameter approximation. The addition of heat flux sensors to quantify actual heat losses are recommended for absolute measurement certainty.

Keywords: T-history, phase change, convective heat transfer.

1. Introduction

There is an ever increasing demand for energy due to global growth and societal development. The need for long term sustainability in energy supply options is self-evident. To achieve this, it is critical to integrate renewable resources into existing energy mixes. A major issue with these options are the intermittency of supply and the misalignment with peak demand. One option to solve this problem is through energy storage. This will allow current systems operating at optimal efficiency to supply constant base load needs and potentially in the future enable renewables to fulfil this function.

Thermal energy storage has been under investigation for many years [1,2] as an alternative to battery based chemical energy storage. Specifically phase change materials (PCMs) have emerged as a low cost option to achieve very high energy density in a wide variety of applications [3,4]. Latent heat thermal energy storage (LHTES) has the potential benefit of energy supply at effectively constant temperature, making it attractive for use in building heating and steam generation.

Research has increased the number of available phase change materials significantly over the years [5,6]. However a major challenge still remains, namely the low thermal conductivity of these materials [7,8]. Many potential solutions have been proposed to overcome this issue, largely focused on the development of composites [9-15]. These composites and in some cases the PCMs themselves are inhomogeneous which makes accurate thermal property measurement difficult [16-18]. To effectively design and size systems it is essential that these property measurements are representative and repeatable.

Traditionally differential scanning calorimetry (DSC) is used to measure properties such as heat capacity and enthalpy of fusion. However, the small size of DSC samples, typically 10-50 mg, makes obtaining representative results for composites difficult. In addition DSC can be very expensive and running one sample at a time, using a proposed scan rate of 0.5 $K.min^{-1}$ for PCMs [19], can become extremely time consuming. For these reasons the *T*-history method [20] and its variations were developed. The approach is very cheap and simply measures the temperature of a sample and reference material, most commonly water, over time. This single measurement can, in theory, be used to calculate the heat capacity, enthalpy of fusion and thermal conductivity of a sample.

Unfortunately the simplicity of the measurement and the lack of a standardized methodology have led to a proliferation of alternatives and adaptations [21-27], both in terms of the setup used and the manner in which the data is employed to obtain the final property values [28]. This in turn presents an abundance of options for measurement but no clear method for distinguishing between the quality and accuracy of the techniques. Most approaches include a simultaneous correction step to ensure agreement with a reference material, but very few, if any, rigorously consider the fundamental validity of the measurement model and its associated assumptions.

While the suggested methods have been catalogued and reviewed [28], no study has as of yet demonstrated an unambiguous basis for selection of the optimal approach. The objective of this investigation is to discern between the wide variety of proposed modifications by formulating them on a common basis. In conjunction their validity will be assessed based on a key assumption of the *T*-history method: the suitability of the natural convection heat transfer coefficient of the reference material to accurately represent the heat loss experienced by the sample. This work uses numerical simulations and experimental measurements to demonstrate the issues associated with the original *T*-history method and its variations. Lastly the approach is recommended which circumvents these identified shortcomings. This work may serve to focus research on developing a rapid measurement technique which utilizes a more fundamentally sound basis.

2. Review of *T*-history method variants

2.1. The original *T*-history method

The original *T*-history method [20] was aimed at simultaneously measuring the melting point, heat capacity, enthalpy of fusion, and thermal conductivity of several samples in a single experiment. It is based on the derivation of a model for the situation where a test tube containing the material in question is at a uniform initial temperature (T_0) and is subsequently exposed to a lower atmospheric temperature (T_∞). It is stated that the atmospheric temperature can be time dependent; however, this refers to the free stream or bulk temperature of the atmosphere. It is explicitly mentioned that if the Biot number is less than 0.1 the temperature distribution in the sample can be neglected and the lumped capacitance method can be used. The rest of the derivation is based on this assumption. It is stated that for natural convection a

heat transfer coefficient of 5-6 $W \cdot m^{-2} \cdot K^{-1}$ can be expected. Also all *salt hydrates* have a stated thermal conductivity greater than 0.3 $W \cdot m^{-1} \cdot K^{-1}$, which satisfies the Biot number condition. Using the measured temperature of the sample ($T(t)$) as it cools, the amount of energy leaving the system can be calculated as:

$$\Delta E = \int_{t_0}^{t_f} A_t h(T(t) - T_\infty) dt = \left(T_0 - T_f\right)\left(m_t c_{p,t} + m_{sa} c_{p,sa}\right) \qquad (1)$$

where h is defined as the *natural or free* convective heat transfer coefficient of air, A_t is the outside area of the tube, T_f is the final measured temperature and the subscripts t and sa refer to the test tube and the sample respectively. It should be noted that in the original derivation, it is not explicitly stated, but since the convective heat transfer coefficient (h) is immediately moved outside of the integral it was implicitly assumed to be constant over the entire time period. The assumptions made regarding the heat transfer coefficient and the heat losses are crucial to the validity of the overall approach.

The same equation (1) is applied to both the sample, PCM, and the reference, usually distilled water. However, the time frames, over which the integration is done, are split differently. For the PCM three segments are defined: from time = 0, at the start of the experiment to t_1, at the start of the phase change process (at which point the temperature is denoted T_s or T_m depending on whether sub-cooling occurs or not). Then from t_1 to t_2, at the end of the phase change process and finally from t_2 to t_3, which is an arbitrary time after solidification has concluded until the sample reaches what is called the reference temperature, or to avoid confusion the final temperature (T_f).

The exact position at which the phase change process is deemed to have ended is not precisely defined and depends on the operator. For this reason some researchers [21] have suggested a more analytical definition of this point. On the other hand for the reference only two segments are defined, the first from time = 0, at the start of the experiment to t'_1, which is the time taken for the reference to cool down to the *temperature* at which phase change starts (T_m or T_s). This may be different from the time taken for the sample to reach this point. The second period runs from t'_1 to t'_2, which is the time taken for the reference to reach the final temperature.

To keep the following derivations simple it is assumed that the PCM does not sub-cool and the phase change occurs at constant temperature (T_m), i.e. an ideal

thermodynamic transition. This neglects any sensible cooling experienced by the test tube during a test run. By taking the ratio of equation (1) for the sample and reference, over the first time period, one obtains:

$$\frac{\int_0^{t_1} A_{t,p} h_p \left(T_p(t) - T_\infty\right) dt}{\int_0^{t'_1} A_{t,r} h_r (T_r(t) - T_\infty) dt} = \frac{\left(T_{0,p} - T_{m,p}\right)\left(m_{t,p} c_{p,t} + m_p c_{p,p}\right)}{\left(T_{0,r} - T_{m,r}\right)\left(m_{t,r} c_{p,t} + m_r c_{p,r}\right)} \qquad (2)$$

where subscripts p and r denote the PCM and reference respectively. It may then be assumed that the two test tubes are identical both in terms of geometry (A_t) and weight (m_t). Furthermore the sample and reference are both heated to the same starting temperature. As noted the time interval, t'_1, is chosen such that the reference temperature at this time is equal to the phase transition temperature of the sample ($T_{m,r} = T_{m,p}$), thus equation (2) simplifies to:

$$\frac{\int_0^{t_1} A_t h_p \left(T_p(t) - T_\infty\right) dt}{\int_0^{t'_1} A_t h_r (T_r(t) - T_\infty) dt} = \frac{\left(m_t c_{p,t} + m_p c_{p,p}\right)}{\left(m_t c_{p,t} + m_r c_{p,r}\right)} \qquad (3)$$

The L.H.S. of equation (3) represents the ratio of the heat lost from the sample and the reference over two similar time periods (since there is no sub-cooling) through convection. Unless the heat transfer coefficient is somehow measured over time for both sample and reference it is clear that these two integrals can be evaluated *if and only if* two primary assumptions are valid:

1. The heat transfer coefficients are both *constant* over the respective time intervals.
2. The heat transfer coefficients are both *equal.*

When these two assumptions are satisfied, equation (3) may be simplified to the final equation given in the original derivation for the modelled liquid heat capacity of the sample:

$$c_{p,l} = \frac{\left(m_t c_{p,t} + m_r c_{p,r}\right)}{m_p} \frac{\int_0^{t_1} \left(T_p(t) - T_\infty\right) dt}{\int_0^{t'_1} (T_r(t) - T_\infty) dt} - \frac{m_t c_{p,t}}{m_p} = \frac{\left(m_t c_{p,t} + m_r c_{p,r}\right)}{m_p} \frac{A_1}{A'_1} - \frac{m_t c_{p,t}}{m_p} \qquad (4)$$

Here A_1 and A'_1 represent the integrals of temperature *only*. During the phase change, the energy change of the sample is more correctly described by:

$$\Delta E = \int_{t_0}^{t_f} A_t h (T(t) - T_\infty) dt = m_p H_m \qquad (5)$$

where H_m is the enthalpy of fusion. In this case the ratio of the expressions for sample and reference (for the same time interval as before) are:

$$\frac{\int_{t_1}^{t_2} A_t h_p\left(T_p(t) - T_\infty\right)dt}{\int_0^{t'_1} A_t h_r(T_r(t) - T_\infty)dt} = \frac{m_p H_m}{(T_0 - T_m)\left(m_t c_{p,t} + m_r c_{p,r}\right)} \quad (6)$$

Again it is clear that the only way to evaluate the integrals is if the previously asserted two assumptions regarding the heat transfer coefficient are satisfied. If this is done one arrives at the final model expression for the enthalpy of fusion:

$$H_m = \frac{\int_{t_1}^{t_2}\left(T_p(t) - T_\infty\right)dt}{\int_0^{t'_1}(T_r(t) - T_\infty)dt} \frac{(T_0 - T_m)\left(m_t c_{p,t} + m_r c_{p,r}\right)}{m_p}$$

$$= \frac{(T_0 - T_m)\left(m_t c_{p,t} + m_r c_{p,r}\right)}{m_p} \frac{A_2}{A'_1} \quad (7)$$

In this case A_2 represents the additional integral. In the original paper [20] equation (7) contains an additional term which accounts for sensible energy lost from tube. This is only relevant if the phase transition does not occur at constant temperature.

For equation (6) the integrals again represent the heat lost from the sample and reference but in this case the two time periods are less closely related than for equation (3). Thus, for arguably this most important property enthalpy, the original method not only assumes the convective heat transfer coefficients for these different and arbitrary time frames are constant but also exactly equal. The experimental rig used in the original investigation is defined as glass test tubes with a diameter of 10.4 mm and height of 180.6 mm. The thermocouple diameter is given as 0.7 mm and the tip is placed 108 mm from the top of the test tube.

2.2. Methods assuming a constant heat transfer coefficient as a function of temperature

One of the earliest modifications was proposed by Marín et al. [22] and the mathematical analysis is slightly different. In this case the same energy balance is done as before, again for both the sample and reference and the ratio is taken. Most significantly however, this is done over a "very small interval", the exact size of which is not mentioned. The interval is stated as being over a small change in the temperature ΔT_i, which has the same size for both sample and reference. It is not explicitly mentioned but it may be assumed that this delta temperature is measured at

the point in time where the sample and reference are at the same temperature. This is based on the fact that all heat capacities used are stated as being at the same temperature (T_i) and two non-identical time periods are used (Δt_i and $\Delta t'_i$). The latter implies that while the change in temperature is identical, it can occur over different time periods for sample and reference. In addition, instead of using the heat capacities and the enthalpy of fusion as done previously, the balance is simply done using specific enthalpy directly, thereby incorporating both prior quantities into a single value. Thus the original equation (2) is modified to:

$$\frac{\int_{t_i}^{t_i+\Delta t_i} A_{t,p} h_p \left(T_{p,i} - T_\infty\right) dt}{\int_{t'_i}^{t'_i+\Delta t'_i} A_{t,r} h_r \left(T_{r,i} - T_\infty\right) dt} = \frac{m_p \Delta H_i}{(T_i - T_{i+1})\left(m_{t,r} c_{p,t} + m_r c_{p,r}\right)} \qquad (8)$$

The same assumptions can be made regarding the tubes as before. This looks similar to the original, however, by choosing the temperature interval for both sample and reference to occur at the same absolute temperature, the two primary assumptions required to complete the integration are modified to:

1. The heat transfer coefficients are both constant over the small time intervals, Δt_i and $\Delta t'_i$.
2. The heat transfer coefficients are both equal *when measured at the same temperature*.

In which case the equation can be simplified and rearranged to give the system model:

$$\Delta H_i = \frac{\int_{t_i}^{t_i+\Delta t_i} \left(T_{p,i} - T_\infty\right) dt}{\int_{t'_i}^{t'_i+\Delta t'_i} \left(T_{r,i} - T_\infty\right) dt} \frac{\left(m_t c_{p,t} + m_r c_{p,r}\right) \Delta T_i}{m_p} = \frac{\Delta T_i \left(m_t c_{p,t} + m_r c_{p,r}\right)}{m_p} \frac{A_i}{A'_i} \qquad (9)$$

Similarly to the original derivation the published version of equation (9) also contains a term which accounts for the sensible energy lost from the tube if the phase transition does not occur at constant temperature. It should be noted that for materials undergoing a thermodynamically ideal phase transition or similar, the approach implies that the heat transfer coefficient for the reference at virtually a single instance in time is identical to that of the sample over its entire phase change period. The reason is that the phase transition occurs at reasonably constant temperature over a long time period while this temperature change occurs for the reference over a much shorter time.

This was one of the first experimental measurements to be conducted in a "motionless" enclosed air chamber (size not given) with a specified maximum temperature change of < 1 ºC. The experimental rig used is defined as glass test tubes with an inner diameter of 10 mm, thickness of 1 mm, and height of 250 mm. The thermocouple thickness is given as 0.127 mm.

A related experimental methodology was proposed by Sandnes and Rekstad [23]. In this case three heated reference samples are placed *on* an insulating polystyrene square. The reduction in temperature is measured; the heat loss rate is calculated for each and averaged. Then, a polynomial fit of the heat loss rate is made as a function of temperature. Three PCM samples are then subjected to the same procedure under identical conditions. The previously determined function is used to calculate the heat lost from the sample at any given temperature and the energy balance is performed to determine the enthalpy change of the sample. This is also done over short time intervals, stated as being equal to the sampling interval. Thus instead of taking the ratio of the heat loss from the sample and reference, the heat loss rate from the reference is substituted directly into the energy balance for the sample, but only at a given temperature.

This is very similar to the prior method where the heat transfer coefficients at a given temperature are assumed to be equal and thus by implication the heat loss rates. If the integration required in equation (9) is done at identical temperature values (T_i) and for the same incremental changes (ΔT_i) in sample and reference, the ratio of A_i and A'_i reduces to a ratio of the time intervals Δt_i and $\Delta t'_i$. Thus equation (9) becomes:

$$\Delta H_i = \frac{\Delta T_i \left(m_t c_{p,t} + m_r c_{p,r}\right)}{m_p} \frac{\Delta t_i}{\Delta t'_i} \quad (10)$$

This can be restated as:

$$\Delta H_i = \frac{\Delta T_i \left(m_t c_{p,t} + m_r c_{p,r}\right)}{\Delta t'_i} \frac{\Delta t_i}{m_p} = \frac{\dot{Q}_{loss,i} \Delta t_i}{m_p} \quad (11)$$

where $\dot{Q}_{loss,i}$ is the heat loss rate of the reference sample at the temperature T_i over the time interval $\Delta t'_i$. This is identical to the model expression given by Sandnes and Rekstad with the exception that the sensible energy changes of the test tube (similar to both prior methods) and that of the sensor are subtracted from $\dot{Q}_{loss,i}$. The reason for the latter is the use of a significantly larger thermocouple (diameter = 12 mm)

compared to the prior experiments. In addition, the test tubes used have a diameter of 31.6 mm and height of 107 mm. It is stated that the heat loss from the tube is independent of the contents; however, similarly to Marín et al. [22] the approach implies that the heat loss rate (or convective heat transfer coefficient) measured for the reference at a specific instance in time is valid for the sample across the entire solidification period.

2.2. Methods assuming a constant heat transfer coefficient as a function of time

A slightly opposing approach to the prior two was suggested by Kravvaritis et al. [24,29]. The experimental setup is similar to Marín et al. [22], with the exception that the container is actively heated and cooled. It should be noted that the heat transfer coefficient referenced and calculated [29] in this investigation [30,31] is for free or natural convection. This is not strictly valid for the experimental setup used since a heating/cooling source will inevitably lead to forced convection in addition to the natural convection caused by the test tubes. Instead of doing the energy balance for a time period where the temperature of the sample and reference are the same, as done previously, the energy balance is now done at the same instance in time. Thus equation (8) can be restated, but using effective heat capacity instead of enthalpy, as:

$$\frac{\int_{t_i}^{t_i+\Delta t_i} A_{t,p} h_p \left(T_{p,i}(t_i) - T_\infty\right) dt}{\int_{t_i}^{t_i+\Delta t_i} A_{t,r} h_r \left(T_{r,i}(t_i) - T_\infty\right) dt} = \frac{m_p c_{p\,eff,i} \left(T_{i,p} - T_{i+1,p}\right)}{\left(T_{i,r} - T_{i+1,r}\right)\left(m_{t,r} c_{p,t} + m_r c_{p,r}\right)} \qquad (12)$$

The same assumptions can be made regarding the tubes as before. For this case the temperature values of the sample and reference are completely unrelated, thus the two primary assumptions required to complete the integration are modified to:

1. The heat transfer coefficients are both constant over the small time interval Δt_i.
2. The heat transfer coefficients are both equal *when measured at the same instance in time*.

In addition, it is assumed that the integral can be calculated numerically using the trapezoidal rule:

$$\int_a^b f(x)dx = \frac{(b-a)[f(a) + f(b)]}{2} \qquad (13)$$

263 Substituting into equation (12):

$$\frac{\Delta t_i\left[\left(T_{i,p}-T_\infty\right)+\left(T_{i+1,p}-T_\infty\right)\right]/2}{\Delta t_i\left[\left(T_{i,r}-T_\infty\right)+\left(T_{i+1,r}-T_\infty\right)\right]/2}=\frac{m_p c_{p\,eff}\left(T_{i,p}-T_{i+1,p}\right)}{\left(T_{i,r}-T_{i+1,r}\right)\left(m_t c_{p,t}+m_r c_{p,r}\right)} \quad (14)$$

264 This can be rearranged to give the system model:

$$c_{p\,eff,i}=\frac{\Delta t_i\left[\left(T_{i,p}-T_\infty\right)+\left(T_{i+1,p}-T_\infty\right)\right]/2}{\Delta t_i\left[\left(T_{i,r}-T_\infty\right)+\left(T_{i+1,r}-T_\infty\right)\right]/2}*\frac{\left(T_{i,r}-T_{i+1,r}\right)\left(m_t c_{p,t}+m_r c_{p,r}\right)}{m_p\left(T_{i,p}-T_{i+1,p}\right)}$$

$$=\frac{\left(m_t c_{p,t}+m_r c_{p,r}\right)\left(T_{i,r}-T_{i+1,r}\right)}{m_p\left(T_{i,p}-T_{i+1,p}\right)}\frac{dA_{i,p}}{dA_{i,r}} \quad (15)$$

265 where $dA_{i,p}$ and $dA_{i,r}$ represent the approximated integrals. This is the equation given
266 by the researchers but with the exclusion of the change in sensible heat of the tube
267 during phase change and the use of non-identical surface areas for the tubes. The data
268 visualization is formulated in terms of "an effective thermal capacity function", which
269 is in reality the temperature derivative of the enthalpy. An equivalent value can be
270 obtained by dividing the calculated enthalpy change across the interval, equation (9),
271 by the temperature change across the interval, giving:

$$c_{p\,eff,i}=\frac{\left(m_t c_{p,t}+m_r c_{p,r}\right)}{m_p}\frac{A_i}{A'_i} \quad (16)$$

272 In this approach the heat transfer coefficient during the entire phase change time
273 period is not assumed to be an approximately constant value (calculated from the
274 reference) as in prior two investigations. Instead it is equal to the value acting on the
275 water tube at the same instance in time, irrespective of the sample and reference
276 temperatures.

277 An approach which avoids integration altogether was suggested by Moreno-
278 Alvarez et al. [25]. Instead of doing the energy balance across a tangible time interval,
279 this approach does the balance for an infinitesimally small time period. In this case
280 the energy balance equation could be rewritten as:

$$\lim_{\Delta t\to 0}\frac{\Delta E}{\Delta t}=A_t h(T(t)-T_\infty)=\lim_{\Delta t\to 0}\frac{\Delta T}{\Delta t}\left(m_t c_{p,t}+m_p c_{p,p}\right) \quad (17)$$

281 This can again be done for both sample and reference and the ratio taken to
282 provide:

$$\frac{A_{t,p}h_p\left(T_p(t)-T_\infty\right)}{A_{t,r}h_r(T_r(t)-T_\infty)}=\frac{\lim_{\Delta t\to 0}\frac{\Delta T_p}{\Delta t}\left(m_{t,p}c_{p,t}+m_p c_{p,p}\right)}{\lim_{\Delta t\to 0}\frac{\Delta T_r}{\Delta t}\left(m_{t,r}c_{p,t}+m_r c_{p,r}\right)} \quad (18)$$

This can be rewritten as:

$$c_{p,p} = \frac{\lim_{\Delta t \to 0} \frac{\Delta T_r}{\Delta t} A_{t,p} h_p \left(T_p(t) - T_\infty\right)}{\lim_{\Delta t \to 0} \frac{\Delta T_p}{\Delta t} A_{t,r} h_r (T_r(t) - T_\infty)} * \frac{\left(m_{t,r} c_{p,t} + m_r c_{p,r}\right)}{m_p} \quad (19)$$

Equation (19) is equivalent to the one provided by the authors with the exception that the sensible energy of the sample tube is not accounted for. In the paper it is stated that, provided the tube areas are close to equal, the heat transfer coefficients may be taken as equal. Practically however, in order to compute equation (19) an assumption must be made whether to calculate the two temperature gradients in the equation at the same point in time or when the temperatures are equal. It is never explicitly mentioned but since experimental data is invariably collected as a time series progression it is logical to assume that the differentials are approximated at the same point in time. By implication the primary assumptions for this method are the same as for Kravvaritis et al. [24]. If the sampling interval is small the differential can approximated as the change over the sampling interval:

$$\frac{\lim_{\Delta t \to 0} \frac{\Delta T_r}{\Delta t}}{\lim_{\Delta t \to 0} \frac{\Delta T_p}{\Delta t}} = \frac{\left(T_{i+1,r} - T_{i,r}\right)/\Delta t_i}{\left(T_{i+1,p} - T_{i,p}\right)/\Delta t_i} \quad (20)$$

This can be substituted into equation (19). It is then easy to show that, if one assumes that the temperature value for that interval is the average of the current and next values, $T_p\,(t) = (T_{i,p}+T_{i+1,p})/2$, equation (19) is in fact identical to equation (15). No detail on the experimental setup is given since only data sets from prior studies are used.

2.3. Methods assuming a negligible heat transfer coefficient

A novel study was conducted by Lázaro et al. [26] at ZAE-Bayern. In this investigation, an insulated enclosure is also used but with some very specific modifications. Firstly, the interior air is heated or cooled using a heat exchanger and a fan to provide forced convective circulation. Secondly, the samples are housed in insulated containers. The dimensions of the enclosure and sample containers are not given. However, it is stated that the sample container is constructed such that the sample is heavily insulated. This fact, coupled with the forced convection inside the

enclosure, makes the insulation the dominant thermal resistance in the system. Thus, the convective heat transfer coefficient becomes largely irrelevant in the analysis.

Unfortunately detail is not given on the mathematical model and data analysis technique used. However, the experimental setup makes it highly likely that the heat loss of the reference at a certain temperature is assumed to be equal to that of the sample at the same temperature. While similar to earlier methods, this however implies the assumption that the thermal conductivity of the reference insulation is equal to that of the sample, not the convective heat transfer coefficients.

A similar approach was recently proposed by Badenhorst [27]. In this case, a cubic polystyrene container (13x13x13 cm) with low thermal conductivity (0.024 $W \cdot m^{-1} \cdot K^{-1}$) is used. A cavity (3x3x3 cm) inside the container is filled with PCM, which is resistively heated and allowed to cool very slowly whilst measuring the temperature at the core and outer edge of the PCM. The container was suspended in air to avoid thermal contact with any surface. A rigorous fundamental model of the system was developed to predict the cooling behaviour. This can be used to determine the melting point, heat capacity, enthalpy of fusion, and thermal conductivity of a given sample.

The exterior of the container is assumed to be at ambient temperature (measured throughout the experiment) and thus the convective heat transfer is not relevant. This work demonstrated that a large temperature gradient can develop between the core and outer edge of the PCM even during extremely slow cooling. The approach has the added advantage of not requiring a reference sample. This is made possible by fully accounting for heat losses from the system through an accurate conduction model.

Additionally, recent work by Tan et al. [32] has demonstrated that, due to the transient nature of the measurement, it is also critical to consider the thermal mass of the insulation during such measurements.

3. Methods and calculations

Two basic experiments were done to provide the data required for the estimation of the convective heat transfer coefficient during a typical *T*-history method test. First, a test tube was filled with distilled water and heated in a lab convection oven to a set temperature. The tube was then exposed to ambient air and allowed to cool. This is done by placement on a flat polystyrene base (thermal conductivity: 0.024 $W \cdot m^{-1} \cdot K^{-1}$)

in a large open room. This is very similar to the experimental setup of Sandnes and Rekstad [23]. A variety of test tubes were tested in this configuration, with dimensions given in Table 1.

Table 1: Dimensions of test tubes used in the experimentation

Length (mm)	150	153	113
Inner Diameter (mm)	15	24	28
Thickness (mm)	1	1	2

The temperature of the fluid was measured using a thermocouple located at the centre of the test tube. A variety of thermocouples were tested with diameters of 6, 1.5 and 0.2 mm, respectively. The ambient air was also measured and both signals digitally sampled. Every combination of tube and thermocouple were tested. During the second test, two identical test tubes were filled with liquids and heated in an oven to a predetermined temperature. The two tubes were then exposed to ambient air and allowed to cool, by placement on a wooden test tube rack in a large open room. The tubes were located 40 mm apart and were either both filled with distilled water or one filled with water and one with ethanol. The same configuration is used to generate *T*-history data for a PCM, myristic acid, using distilled water as reference. Myristic acid (CAS 544-63-8) with a purity >95% was obtained from Sigma-Aldrich.

Numerical simulation was done in the commercial package ANSYS Fluent ®. Fluids were modelled as constant density while the ambient air was modelled using the ideal gas law. This captures natural convection in the air space but neglects such movement in the fluid within the tube. The exception is when modelling the PCM, in which case the Boussinesq approximation is used. This accounts for the body force experienced by the fluid phase due to buoyancy. Simulations are conducted in double precision and the convergence limits on continuity (and velocity) and energy are 0.001 and $1x10^{-6}$, respectively. The PRESTO! algorithm and SIMPLE scheme are used for pressure spatial discretization and the pressure-velocity coupling. Grid size is varied from 1 mm intervals at the test tube up to 20 cm at the edges of the container depending on its size. Flow is assumed to be laminar and Newtonian while thermos-physical properties are assumed constant.

A variety of physical configurations were examined. As an ideal case (A) a small test tube (glass) filled with fluid (water) was simulated as being suspended in a large open room (10x10x10 m). All simulated test tubes had the dimensions of those used in the investigation by Marín et al. [22]: inner diameter of 10 mm, thickness of 1 mm and height of 250 mm. In the second simulation (B) the test tube is placed on a flat, wooden table to represent this potential airflow obstruction. Finally, (C.i) the tube is placed inside a square container (50x50x50 cm). These designs are shown schematically in Figure 1.

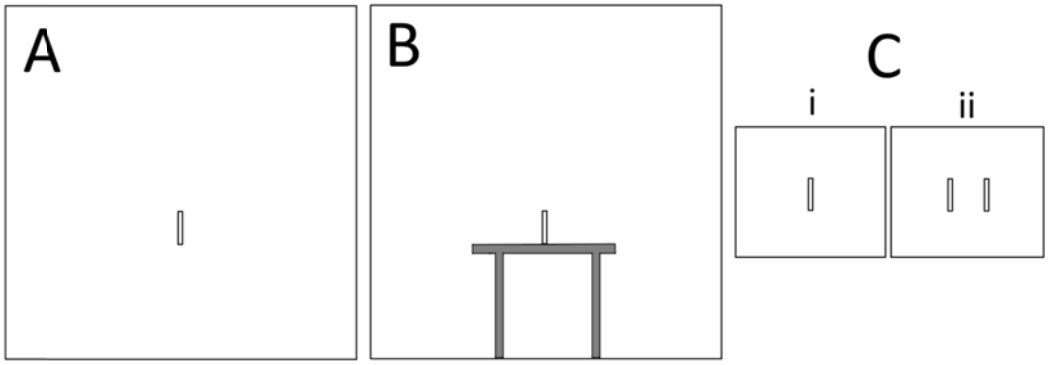

Fig. 1: Simulation configurations.

The last configuration was expanded as shown to include two tubes (C.ii). For this arrangement the fluids in the tubes are varied in a similar fashion to the experimental investigation: either both filled with distilled water or one filled with water and one with ethanol.

4. Results and discussion

The simulation was validated using configuration (B) and the experimental data for a single tube filled with distilled water. During validation only the tube geometry and starting temperatures are changed to correspond with the specific experiment. Shown in Figure 2 is the predicted cooling curve and experimental result for cooling of distilled water from 55 ºC.

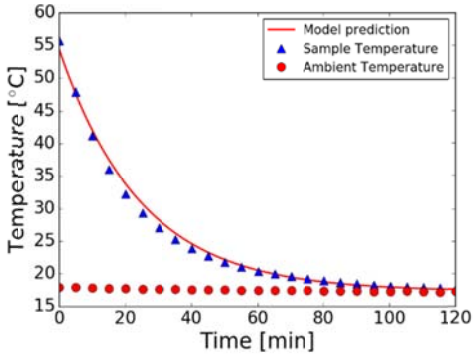

Fig. 2: Simulation validation using experimental results.

The prediction agrees well with the experimental results indicating that the simulation accurately represents the sample and its heat loss over time. The simulation is further validated against the data from Sandnes and Rekstad [23] also using configuration (B). In this case the averaged cooling data of the water reference samples are compared to the predicted response.

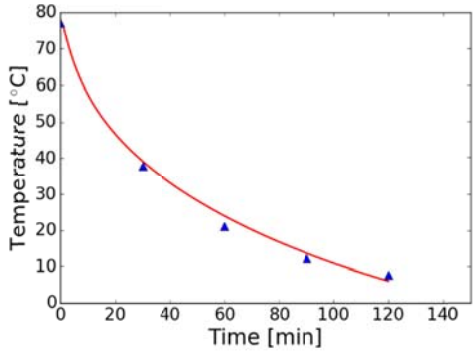

Fig. 3: Simulation validation using results of Sandnes and Rekstad [23].

The fit is good but a deviation from the measurement is visible. The reason for this is a noticeable drift in the ambient temperature as seen in the experimental data. The lumped parameter or lumped capacitance model forms an integral part of most of the preceding techniques. This model is derived for an arbitrarily shaped body which is heated to a homogenous starting temperature and then allowed to cool in a fluid. It is important to note that a basic assumption of the model is that the body is homogenous and a solid. In no way does the analysis include a change of phase with its associated energy release, nor does it include the presence of both a solid and liquid phase within the body. Nonetheless, based on the assumption that the body

experiences an extremely small temperature gradient, a transient energy balance can be done to yield the expression:

$$\frac{T(t)-T_\infty}{T_0-T_\infty}=e^{\left(-hA_st/\rho C_pV\right)} \qquad (21)$$

The derivative of this expression with respect to time is:

$$\frac{1}{T_0-T_\infty}\frac{dT(t)}{dt}=\left(\frac{-hA_s}{\rho C_pV}\right)e^{\left(-hA_st/\rho C_pV\right)} \qquad (22)$$

The ratio of equations (22) and (21) gives:

$$\frac{1}{T(t)-T_\infty}\frac{dT(t)}{dt}=\left(\frac{-hA_s}{\rho C_pV}\right) \qquad (23)$$

This can be rewritten to find:

$$h(t)=\frac{-\rho C_pV}{A_s(T(t)-T_\infty)}\frac{dT(t)}{dt} \qquad (24)$$

If all the assumptions underlying the lumped parameter model are met, a plot of the temporal derivate of the temperature signal divided by the temperature signal itself should give a constant value over time. This value must be equal to the convective heat transfer coefficient, provided the applicable values for the tube geometry, physical properties of the material and the ambient temperature signal are used in the calculation.

The experimental results for the first test, the cooling of single test tube filled with water, are examined based on such a plot of $h(t)$. As mentioned, all possible combinations of tube and thermocouple were explored. However, for clarity and brevity only five representative results are presented in Figure 4. The results are displayed as the convective heat transfer coefficient, calculated using equation (24).

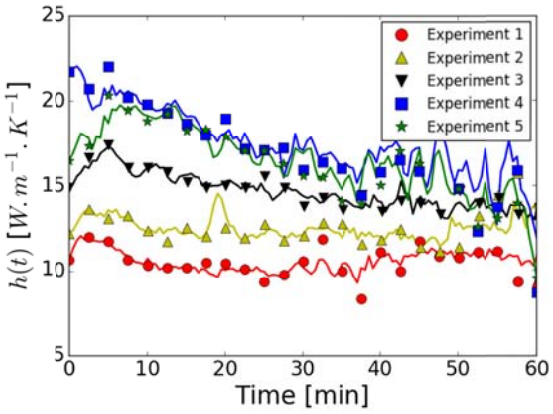

Fig. 4: Experimental results for cooling of single tube filled with water.

The measured convective heat transfer coefficients are not stable over time and undergo substantial fluctuations. This is true for all the experiments conducted. The tests also exhibit a variation up to a factor of 2 in the absolute value of the average heat transfer coefficient, relative to each other. This is not unexpected given the variation in experimental configurations. This demonstrates that it is necessary to have a standardized experimental setup to ensure consistent results.

Across the majority of experiments the heat transfer coefficients exhibit the tendency to decrease over time. In some case as much as a 50% reduction is realized between start and finish. This is due to a reduction in the driving force for generating convective air flow as the tube cools. At an experimental time of 60 minutes all samples are within 10 ºC of ambient. Beyond this point the calculated heat transfer coefficient becomes extremely noisy with large fluctuations. The calculated heat transfer coefficient then carries a very high uncertainty due to the derivative of the temperature signal, which is only changing marginally. Thus, from the experimental data it is clear that the heat transfer coefficient cannot be considered constant across long time periods of time.

To understand why these variations occur it is useful to examine the simulations which represent this and other related scenarios. Simulation configuration (A) represents a somewhat idealized case: a single glass tube suspended in a very large room. There are no physical obstructions, airflow is free to develop and the temperature rise of the air is negligible. This can be verified by a contour plot of temperature as shown below in Figure 5 (A).

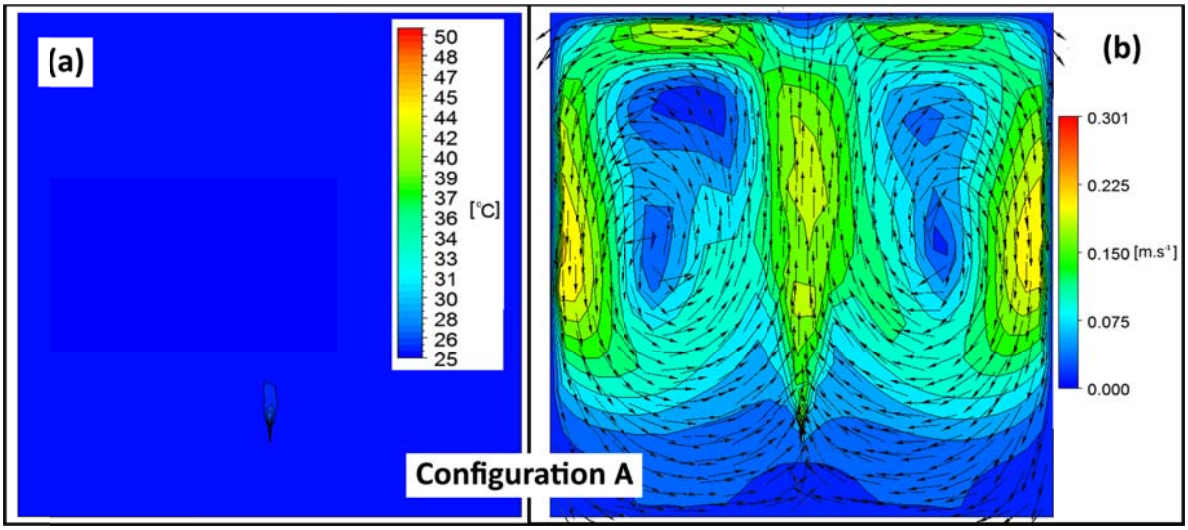

Fig.5: Simulation results configuration (A) after 3 minutes elapsed time: contour plots of (a) temperature and (b) air velocity

After three minutes there has been virtually no change in the room temperature, however the impact on the air circulation is substantial. Two cells have developed and air circulation is highly erratic. In the case of a tube placed on a table, due to the presence of the table structure, the flow patterns are disrupted. This is especially true in the region close to the tube as can be observed in Figure 6.

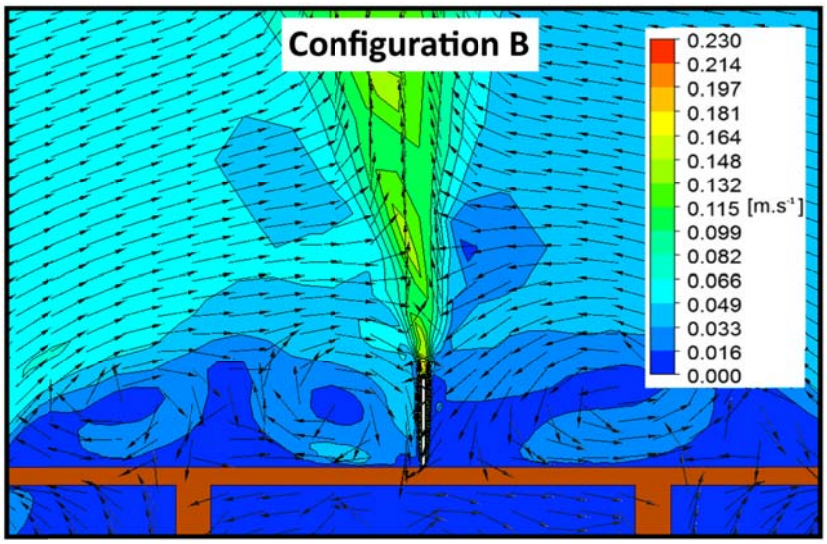

Fig.6: Close-up of table structure in configuration (B) after 3 minutes elapsed time: contour plot of air velocity

Unstable and sporadic vortices form leading to highly erratic flow patterns. These instabilities lead to the fluctuations found in the experimentally determined heat transfer coefficients. The situation is similar for the next case where the test tube is confined to a small container. The predicted system behaviour for this configuration (C.i) is illustrated below in Figure 7.

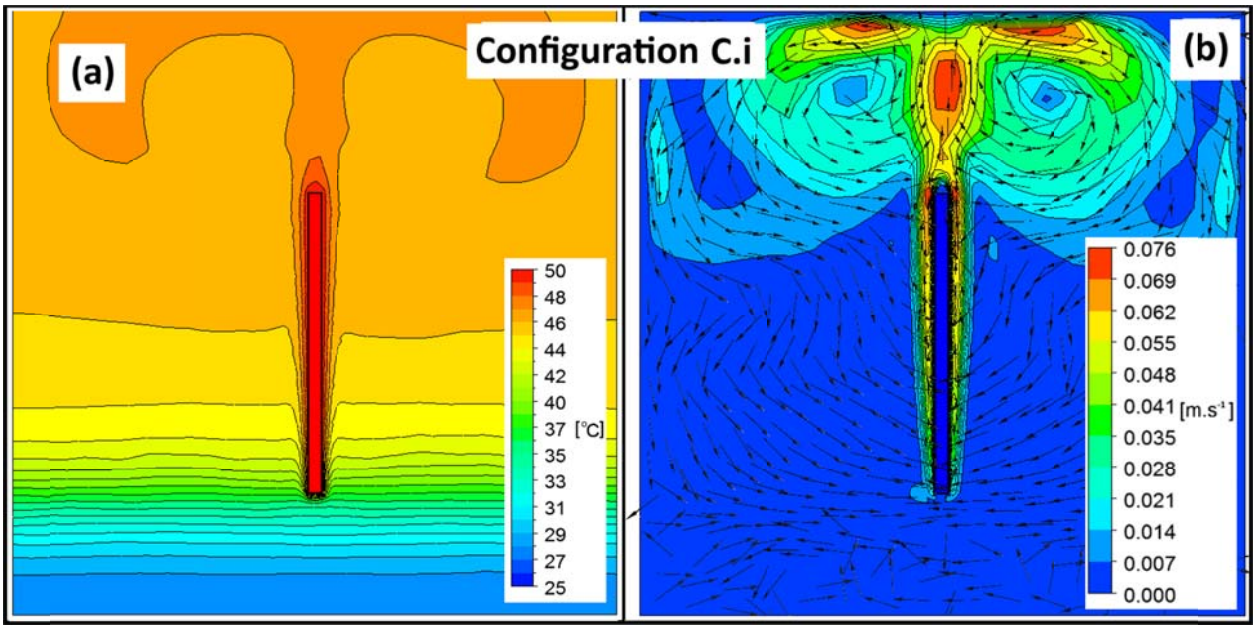

Fig.7: Simulation results configuration (C.i) after 10 minutes elapsed time: contour plots of (a) temperature and (b) air velocity

An erratic airflow develops which is closely related to the prior two cases. Due to the smaller volume of air, the air temperature rises far more rapidly than in the room. Thermal stratification is clearly visible in the container. This result implies that without active heating/cooling it will be very difficult to maintain the temperature change inside the box to less than 1 ºC during cooling.

All three of these configurations indicate that an unstable convective heat transfer coefficient forms under natural convection, as observed experimentally. This is unavoidable due to the nature of the air movement which develops around the test tube. Thus the experimental and simulation results both indicate that it is infeasible to assume that heat transfer coefficients remain constant for extended periods of time. This invalidates the underlying assumptions of the original *T*-method. The limitations of the arbitrary time frames used by the original approach are overcome by all subsequent modifications of the original method examined here. In each case the energy balance between sample and reference is only completed over a short time interval.

The next experimental tests aim to determine whether a reference material, cooling down alongside the sample, can be used to calculate the sample heat loss at a given temperature or point in time. First two identical tubes were filled with distilled

water and subjected to the *T*-history method. The heat transfer coefficients for both tubes exhibited large fluctuations and a gradual decay. However, a definite correlation exists between the two tubes and the time based variations are mutual for both tubes. This is due to interaction of the airflow which develops between the two tubes, as can be demonstrated using the simulation for this case. The velocity contours for a double tube configuration are demonstrated in Figure 8.

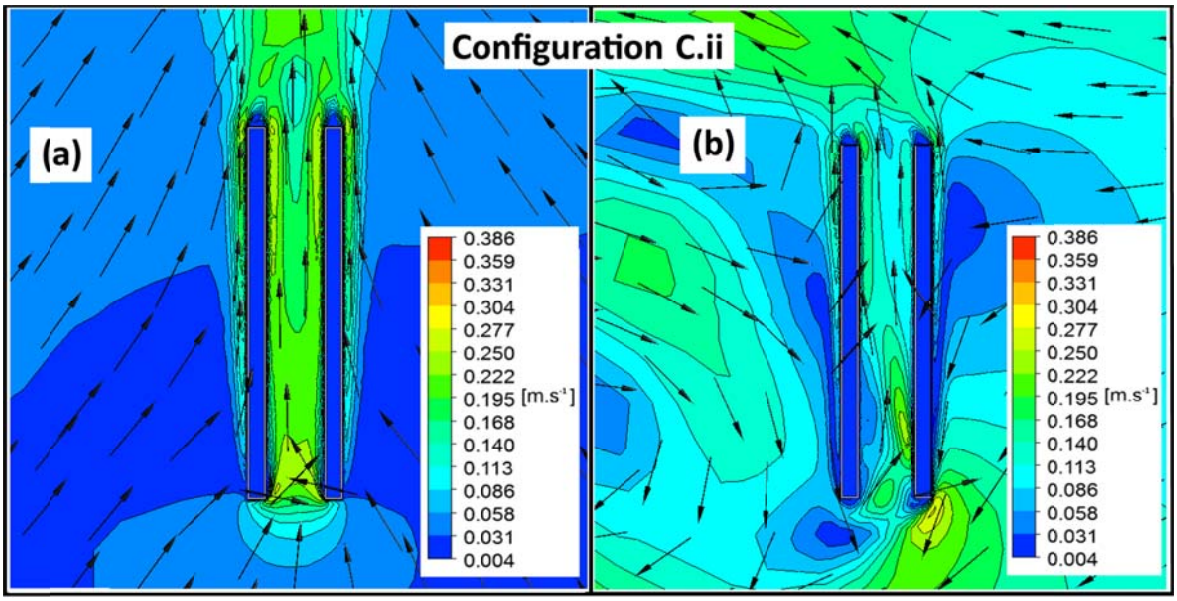

Fig. 8: Simulation contour plots of air velocity for configuration (C.ii) after (a) 3 and (b) 25 minutes elapsed time.

The tubes are in close enough proximity to influence the air flow in the region between them quite differently from the flow on the outside of the tubes. This would also be the case for horizontal tubes. For tubes filled with identical liquids this does actually yield very similar heat transfer coefficients. However, a more realistic case is where the fluids in the tubes have different thermal properties. To represent this situation the test was repeated but with water in one tube and ethanol in the other. The results are given in Figure 9.

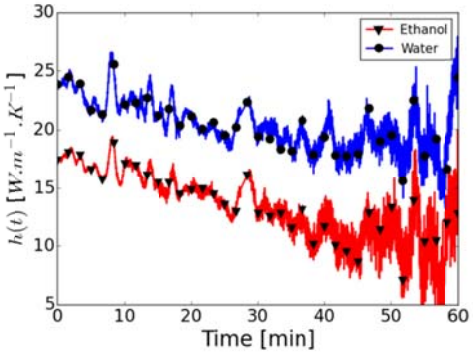

513

515 Fig. 9: Experimental results for cooling of two tubes, one ethanol (a) and one
516 water (b), against time.

516

528 The first noticeable outcome is the fact that at any given time and by implication
529 any given temperature, the calculated heat transfer coefficient values differ. The value
530 for ethanol is significantly lower than water. This is not unexpected if one considers
531 the fact that the water cools far less rapidly than the ethanol. The outer temperature of
532 the water can be higher than the ethanol by more than a factor of two (normalized to
533 ambient). Thus the density of the air in contact with the water tube is significantly less
534 than the ethanol tube, hence the buoyant force and consequently air velocity
535 developed is much higher. This leads to a substantially higher convective heat transfer
536 rate. In fact, if the *T*-history was used to calculate the heat capacity of ethanol using
537 this data set, the estimated value would be 3145 J/kg, an error of 29%. This
538 observation directly invalidates approaches which assume that the heat transfer
539 coefficients are *equal*, whether at the same temperature or point in time.

537 In addition, it was found that this test had poor repeatability. When the experiment
538 is repeated under practically identical conditions the heat transfer coefficients
539 developed are not the identical. This is due to the chaotic nature in which the air flow
540 develops around the tubes. As can clearly be seen from Figure 9, the two signals are
541 correlated in time, meaning they experience similar peaks and valleys at the same
542 moment in time due to their proximate interactions. The implication of this is that
543 when compared at the same temperature, these fluctuations are not coincidental. This
544 is evident from Figure 10, where the heat transfer coefficients are plotted against
545 temperature.

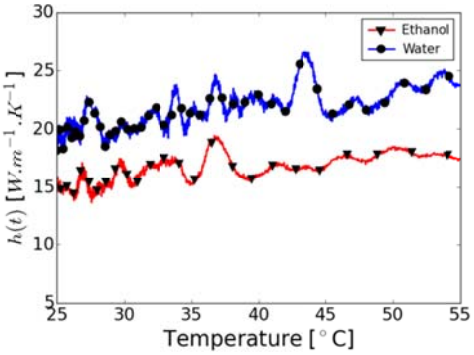

538

540 Fig. 10: Experimental results for cooling of two tubes, one ethanol (a) and one
541 water (b), against temperature.

541

546 The event which temporarily increases both heat transfer coefficients at an
547 experimental time of around 28 minutes, occurs for ethanol at 36 ºC but for water at
548 44 ºC. Thus it is not possible to state that the heat transfer coefficient is a simple
549 function of temperature, such as $h(T) = T^n$, since this expression does not accurately
550 represent the heat transfer coefficient at any given moment.

554 Conversely, the two calculated heat transfer coefficients shown in Figure 9
555 demonstrate an excellent correlation in time. This does not however imply that it is
556 better to assume that the heat transfer coefficients for sample and reference are equal
557 at a given time in the experiment. As already demonstrated the value measured for
558 ethanol is significantly lower compared to water due to differences in temperature and
559 hence driving forces for convection at any given time. This effect is highly
560 exaggerated in the case of phase change materials, as demonstrated by the
561 experimental result for the cooling of a PCM, illustrated in Figure 11.

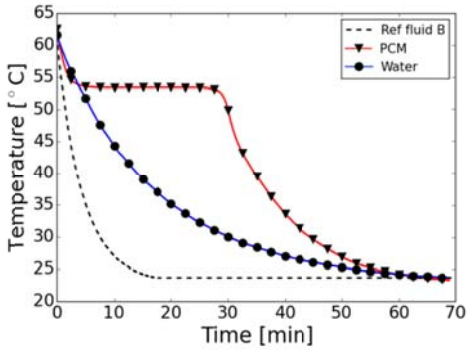

555

556 Fig. 11: Experimental result for PCM cooling

557

The temperature of the PCM remains high during phase change while the reference fluid cools to ambient. An extreme case is demonstrated by Ref fluid B which has significantly lower thermal capacity. It cools rapidly to ambient, resulting in very limited convection around the reference tube after approximately 20 min. By suitable choice of the reference an improved estimate may be achieved, but it would be impossible for the convection coefficients to be equal due to the effect of phase change.

Thus despite the fact that the sample and reference heat transfer coefficients may be correlated both in time and temperature, they cannot be equal at any given time or temperature. Hence there will always be an associated error in every derivation using convective heat losses as part of the calculation through the energy balance. This is true whether the method involves integration [20,22,24] or differentiation [25]. The only way in which this error can be eliminated is by removing it from the computation, as is done in the third class of methods.

To achieve this it may be assumed that the convective resistance of the system should be less than 5% of that of the conductive. Using the standard expressions for these variables [33] it may be shown that for an enclosure using the polystyrene material mentioned earlier [27] (k~0.024 $W.m^{-1}.K^{-1}$), a will thickness of 32 mm would be required. For this case the convective heat transfer coefficient is assumed to be 15 $W.m^{-2}.K^{-1}$ in accordance with the average, measured natural convection values. The thickness can be further reduced if a forced convection setup like the one of Lázaro et al. [26] is used. In this manner the system can be tailor-made for a specific PCM to achieve the optimal cooling rate.

The experimentally determined values for the convective heat transfer coefficients are in the region expected for natural convection 10 - 25 $W \cdot m^{-1} \cdot K^{-1}$ [33]. However, they are notably higher than the range of expected coefficients given by Yinping et al. [20] as 5 - 6 $W \cdot m^{-1} \cdot K^{-1}$. Most *T*-history methods assume validity of the lumped parameter model. To satisfy the Biot number requirement with the current values, materials with thermal conductivities significantly higher than 1 $W \cdot m^{-1} \cdot K^{-1}$ on average would be required, which excludes many PCMs. Furthermore as can be seen from Figure 7, the boundary layer surrounding a tube grows in size, as would be expected, from the bottom to the top. In addition, the linear velocity increases along the tube. This is due to the buoyant force applied to the air, which increases as the air

590 heats up during flow past the tube. As a result of these boundary layer and velocity
591 variations, the convective heat transfer coefficient can vary by up to a factor of three
592 between the top and bottom of the tube.
593 This demonstrates the inaccuracy of using a single heat transfer coefficient for the
594 entire tube. Furthermore, it raises doubts regarding the assumption that the Biot
595 number is satisfied at all positions on the tube for PCM experiments, especially for
596 tubes which have a large aspect ratio. As mentioned, the lumped parameter model
597 was not developed for a system where heat is released. High thermal gradients in the
598 sample have been found experimentally and through detailed modelling [27], in direct
599 contradiction with the use of the lumped parameter model. This conclusion is
600 supported by the recent work of Mazo et al. [34] which clearly demonstrates the effect
601 of radial thermal gradients inside *T*-history samples cannot be neglected. Thus for all
602 of these reasons it is evident that the application of the lumped parameter method
603 should be avoided in favour of more rigorous and accurate representations.
604
605 **5. Conclusions and recommendations**
606 Energy storage remains a key issue in developing a sustainable energy mix. The
607 production of new phase change composite materials for thermal energy storage
608 necessitates accurate and representative measurement of their properties. While the *T*-
609 history method offers a quick and simple solution, it has led to a wide variety of
610 alternatives and adaptions. None of these methods follow a standardized approach and
611 selecting between them has become very difficult.
612 It has been demonstrated that most of these variants can be classified into three
613 distinct classes:
614 1) Methods which assume the convective heat transfer coefficient is equal for
615 sample and reference at the same temperature.
616 2) Methods which assume the convective heat transfer coefficient is equal for
617 sample and reference at the same point in time, since the start of the
618 experiment.
619 3) Methods which assume the convective heat transfer coefficient is negligible,
620 achieved by making conduction the dominant thermal resistance in the system.
621 Both numerical modelling and experimental work have been used to test the
622 validity of the assumptions underlying the first two groups of models. This work has

623 demonstrated that the convective heat transfer coefficients which develop under
624 natural or free convection are highly variable. The primary cause is the random and
625 disordered air flow which develops. It is however clear, that for two different fluids,
626 cooling down under these conditions it can never be stated that the convective heat
627 transfer coefficients are equal.

628 The convective heat transfer coefficients do however, exhibit varying degrees of
629 correlation as a function of both time and temperature. The latter is due to the fact that
630 the temperature of the material in question drives the buoyant force which creates the
631 convective effect. At higher temperatures this effect is increased (lowered air density)
632 and higher convective heat transfer is achieved. However, due to the fact that the air
633 flow zones which develop around the cooling sample and reference are mutually
634 interrelated time based fluctuations manifest on both. Thus, at any given point in time,
635 these random variations can shift the coefficient away from the value expected at a
636 given temperature in both sample and reference.

637 This is particularly problematic for phase change materials in cases where the
638 instantaneous value of the heat transfer coefficient for the reference is used for the
639 entire solidification time period. In addition, if the reference is chosen incorrectly the
640 sample may be undergoing solidification at the melting temperature while the
641 reference has cooled down to ambient. Comparing heat transfer coefficients under
642 such conditions would introduce significant error.

643 Furthermore, it was revealed that significant spatial variation of the heat transfer
644 coefficient occurs on the tube with cross flow effects possible between two tubes.
645 This, in conjunction with other effects such as convective forcing and sample thermal
646 gradients make it clear that a more rigorous model is needed and the lumped
647 parameter approach should not be used. The problem is overcome in the third class of
648 models. In this case conduction is engineered to be the dominant thermal resistance in
649 the system, thereby removing any uncertainty associated with the convective heat
650 transfer coefficient.

651 These systems can be constructed to reduce the experimental time to a minimum
652 for a given PCM composite. Furthermore the system can be fully analysed
653 analytically, thereby making the simultaneous reference sample complimentary rather
654 than required. Therefore, it is recommended that future effort is focused on
655 developing the third class of *T*-history method systems. Additional effort should be

placed on verifying the achieved conduction losses in this configuration through the use of heat flux sensors to physically measure these values. In this manner all factors can be accounted for and the analytical model of the method fully verified.

Acknowledgments

The research leading to these results has received funding from the European Commission Seventh Framework Programme (FP/2007-2013) and under Grant agreement NºPIRSES-GA-2013-610692 (INNOSTORAGE), and from the European Union's Horizon 2020 research and innovation programme under grant agreement No 657466 (INPATH-TES). The work is partially funded by the Spanish government (ENE2015-64117-C5-1-R (MINECO/FEDER)). Dr. Luisa F. Cabeza would like to thank the Catalan Government for the quality accreditation given to the research group GREA (2014 SGR 123).

Nomenclature

All values are in SI standard units

T_m	Melting temperature
$T_{m,p}$	Melting temperature PCM
$T_{m,r}$	Melting temperature reference
T_s	Sub-cool temperature
T_0	Initial temperature
$T_{0,p}$	Initial PCM temperature
$T_{0,r}$	Initial reference temperature
T_f	Final temperature
T_∞	Ambient or atmospheric temperature
$T(t)$	Temperature as a function of time (sample or reference)
ΔT_i	Temperature change at interval i
T_i	Temperature at interval i
T_{i+1}	Temperature at interval i+1
$T_{p,i}$	PCM temperature at interval i
$T_{r,i}$	Reference temperature at interval i

689	T_p	PCM temperature
690	T_r	Reference temperature
691	ΔE	System energy loss
692	t_0	Initial time ($t=0$)
693	t_f	Final time
694	Δt_i	Time change at interval i
695	A_s	Surface area
696	A_t	Heat transfer area (of test tube)
697	$A_{t,p}$	Heat transfer area (of PCM test tube)
698	$A_{t,r}$	Heat transfer area (of reference test tube)
699	h	Convective heat transfer coefficient
700	$h(T)$	Convective heat transfer coefficient as function of temperature
701	h_p	Convective heat transfer coefficient (of PCM test tube)
702	h_r	Convective heat transfer coefficient (of reference test tube)
703	t	Time
704	m_t	Mass of test tube
705	$m_{t,p}$	Mass of reference test tube
706	$m_{t,r}$	Mass of sample test tube
707	m_{sa}	Mass of sample
708	m_p	Mass of PCM
709	m_r	Mass of reference
710	c_p	Heat capacity
711	$c_{p\ eff,i}$	Effective heat capacity of PCM at interval i
712	$c_{p,l}$	Heat capacity of liquid
713	$c_{p,s}$	Heat capacity of solid
714	$c_{p,t}$	Heat capacity of test tube
715	$c_{p,sa}$	Heat capacity of sample
716	$c_{p,r}$	Heat capacity of reference
717	$c_{p,p}$	Heat capacity of PCM
718	H_m	Enthalpy of fusion
719	ΔH_i	Enthalpy change across interval i
720	$\dot{Q}_{loss,i}$	Heat loss at interval i
721	ρ	Density

722 V Volume

723

724 **References**

725 [1] Zalba B, Marín JM, Cabeza LF, Mehlig H. Review on thermal energy storage with
726 phase change: materials, heat transfer analysis and applications. Appl. Therm. Eng.
727 2003;23:251-83.

728 [2] Sharma A, Tyagi VV, Chen CR, Buddhi D. Review on thermal energy storage
729 with phase change materials and applications. Renew. Sustain. Energy Rev.
730 2009;13:318-45.

731 [3] Zhou D, Zhao CY, Tian Y. Review on thermal energy storage with phase change
732 materials (PCMs) in building applications. Appl. Energy 2012;92:593-605.

733 [4] Tian Y, Zhao CY. A review of solar collectors and thermal energy storage in solar
734 thermal applications. Appl. Energy 2013;104:538-553.

735 [5] Khare S, Dell'Amico M, Knight C, McGarry S. Selection of materials for high
736 temperature latent heat energy storage. Sol. Energy Mater. Sol. Cells 2012;107:20-
737 7.

738 [6] Oró E, de Gracia A, Castell A, Farid MM, Cabeza LF. Review phase change
739 materials (PCMs) for cold thermal energy storage applications. Appl. Energy
740 2012;99:513-33.

741 [7] Zeng J, Zheng S, Yu S, Zhu F, Gan J, Zhu L, et al. Preparation and thermal
742 properties of palmitic acid/polyaniline/exfoliated graphite nanoplatelets form-
743 stable phase change materials. Appl. Energy 2014;115:603-9.

744 [8] Xiao X, Zhang P, Li M. Thermal characterization of nitrates and nitrates/expanded
745 graphite mixture phase change materials for solar energy storage. Energy Convers.
746 Manage. 2013;73:86-94.

747 [9] Zhang L, Zhu J, Zhou W, Wang J, Wang, Y. Thermal and electrical conductivity
748 enhancement of graphite nanoplatelets on form-stable polyethylene glycol /
749 polymethyl methacrylate composite phase change materials. Energy 2012;39:294-
750 302

751 [10] Fang Z, Fan L, Ding Q, Wang X, Yao X, Hou J, et al. Increased Thermal
752 Conductivity of Eicosane-Based Composite Phase Change Materials in the
753 Presence of Graphene Nanoplatelets. Energy Fuels 2013;27:4041-7.

754 [11] Badenhorst H, Focke W. Comparative analysis of graphite oxidation behaviour
755 based on microstructure. J. Nucl. Mater. 2013;442:75-82
756 [12] Ji H, Sellan DP, Pettes MT, Kong X, Ji J, Shi L, et al. Enhanced thermal
757 conductivity of phase change materials with ultrathin-graphite foams for thermal
758 energy storage. Energy Environ. Sci. 2014;7:1185–92.
759 [13] Li M, Wu Z, Tan J. Properties of form-stable paraffin/silicon dioxide/expanded
760 graphite phase change composites prepared by sol–gel method. Appl. Energy
761 2012;92:456-61.
762 [14] Fan LW, Fang X, Wang X, Zeng Y, Xiao YQ, Yu ZT, et al. Effects of various
763 carbon nanofillers on the thermal conductivity and energy storage properties of
764 paraffin-based nanocomposite phase change materials. Appl. Energy
765 2013;110:163-72.
766 [15] Badenhorst H, Fox N, Mutalib A. The use of graphite foams for simultaneous
767 collection and storage of concentrated solar energy. Carbon 2016;99:17-25.
768 [16] Asseal MJ, Dix M, Gialou K, Vozar L, Wakeham WA. Application of the
769 Transient Hot-Wire Technique to the Measurement of the Thermal Conductivity of
770 Solids, Int. J. Thermophys. 2002;23:615-33.
771 [17] Jensen C, Xing C, Folsom C, Ban H, Phillips J. Design and Validation of a High-
772 Temperature Comparative Thermal-Conductivity Measurement System, Int. J.
773 Thermophys. 2012;33:311-29.
774 [18] Wulf R, Barth G, Gross U, Intercomparison of Insulation Thermal Conductivities
775 Measured by Various Methods, Int. J. Thermophys. 2007;28:1679-92.
776 [19] Gschwander S, Lazaro A, Cabeza LF, Günther E, Fois M, Chui J. Development
777 of a Test-Standard for PCM and TCM Characterization. Part 1: Characterization of
778 Phase Change Materials. IEA Solar Heating and Cooling / Energy Conservation
779 through Energy Storage programme – Task 42/Annex 24: Compact Thermal
780 Energy Storage, Paris, France; 2011.
781 [20] Yinping Z, Yi J, Yi J. A simple method, the T-history method, of determining the
782 heat of fusion, specific heat and thermal conductivity of phase-change materials.
783 Meas. Sci. Technol. 1999;10:201-5.
784 [21] Hong H, Kim SK, Kim Y-S. Accuracy improvement of T-history method for
785 measuring heat of fusion of various materials. Int. J. Refrig. 2004;27:360–6.

786 [22] Marín JM, Zalba B, Cabeza LF, Mehling H. Determination of enthalpy-
787 temperature curves of phase change materials with the temperature-history method:
788 improvement to temperature dependent properties. Meas. Sci. Technol.
789 2003;14:184–9.
790 [23] Sandnes B, Rekstad J. Supercooling salt hydrates: Stored enthalpy as a function
791 of temperature. Sol. Energy 2006;80:616–25.
792 [24] Kravvaritis ED, Antonopoulos KA, Tzivanidis C. Improvements to the
793 measurement of the thermal properties of phase change materials. Meas. Sci.
794 Technol. 2010;21(045103):9.
795 [25] Moreno-Alvarez L, Herrera JN, Meneses-Fabian C. A differential formulation of
796 the T-History calorimetric method. Meas. Sci. Technol. 2010;21(127001):4.
797 [26] Lázaro A, Günther E, Mehling H, Hiebler S, Marín JM, Zalba B. Verification of
798 a T-history installation to measure enthalpy versus temperature curves of phase
799 change materials. Meas. Sci. Technol. 2006;17:2168–74.
800 [27] Badenhorst H. Performance comparison of three models for thermal property
801 determination from experimental phase change data. Thermochim. Acta
802 2015;616:69-78.
803 [28] Solé A, Miró L, Barreneche C, Matrorell I, Cabeza LF. Review of the T-history
804 method to determine thermophysical properties of phase change materials (PCM).
805 Renew. Sustain. Energy Rev. 2013;26:425-36.
806 [29] Kravvaritis ED, Antonopoulos KA, Tzivanidis C. Experimental determination of
807 the effective thermal capacity function and other thermal properties for various
808 phase change materials using the thermal delay method. Appl. Energy
809 2011;88:4459-619.
810 [30] Popiel CO. Free convection heat transfer from vertical slender cylinders: a
811 review. Heat Transfer Eng. 2008;29:521–36.
812 [31] Popiel CO, Wojtkowiak J, Bober K. Laminar free convective heat transfer from
813 isothermal vertical slender cylinder. Exp. Thermal Fluid. Sci. 2007;32:607–13.
814 [32] Tan P, Brütting M, Vidi S, Ebert HP, Johansson P, Jansson H, Kalagasidis AS.
815 Correction of the enthalpy–temperature curve of phase change materials obtained
816 from the T-History method based on a transient heat conduction model. Int. J. of
817 Heat Mass Tran. 2017;105:573-88.

818 [33] Incropera FP, DeWitt DP, Bergman TL, Lavine AS, Fundamentals of Heat and
819 Mass Transfer, John Wiley & Sons, New Jersey, 2007.
820 [34] Mazo J, Delgado M, Lázaro A, Dolado P, Peñalosa C, Marín JM, Zalba B. A
821 theoretical study on the accuracy of the T-history method for enthalpy–temperature
822 curve measurement: analysis of the influence of thermal gradients inside T-history
823 samples. Meas. Sci. Technol. 2015;26:125001.1:10.
824